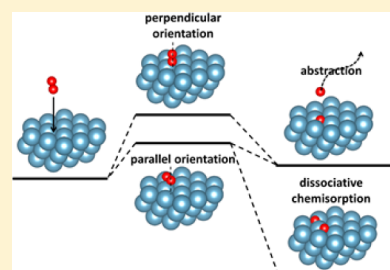


Dissociative Adsorption of O₂ on Al(111): The Role of Orientational Degrees of Freedom

Jin Cheng,[†] Florian Libisch,[‡] and Emily A. Carter^{*,§}[†]Department of Chemistry, Princeton University, Princeton, New Jersey 08544-1009, United States[‡]Institute for Theoretical Physics, Vienna University of Technology, 1040 Vienna, Austria, European Union[§]Department of Mechanical and Aerospace Engineering, Program in Applied and Computational Mathematics, and Andlinger Center for Energy and the Environment, Princeton University, Princeton, New Jersey 08544-5263, United States

Supporting Information

ABSTRACT: The interaction between O₂ molecules and Al surfaces has long been poorly understood despite its importance in diverse chemical phenomena. Early experimental investigations of adsorption dynamics indicated that abstraction of a single O atom by the surface, instead of dissociative chemisorption, dominates at low O₂ incident kinetic energies. Abstraction of the closer O atom suggests low barrier heights at perpendicular incidence. However, recent measurements suggest that parallel O₂ orientations dominate sticking at low energies. We resolve this apparent contradiction by a systematic ab initio embedded correlated wavefunction study of the stereochemistry of O₂ reacting with Al(111). We identify two important new details: (i) initially, roughly parallel oxygen molecules tend to tilt upright while approaching the surface, suggesting that the abstraction channel does dominate at low energies and (ii) the reaction channel with the lowest barrier indeed corresponds to a parallel orientation, which ultimately evolves either into dissociative chemisorption or toward abstraction.



The interaction between oxygen and aluminum is of fundamental importance in phenomena ranging from mineral formation to corrosion to rocket propulsion. However, the mechanism of how aluminum is oxidized is still not fully understood, even for the seemingly simple case of one oxygen molecule interacting with a perfect Al(111) single-crystal surface.¹ Moreover, most theoretical methods have difficulty in describing even this well-defined reaction. For example, the experimentally observed reaction barrier for dissociative chemisorption^{2–4} is absent in conventional density functional theory (DFT) calculations, except for one specific O₂ configuration.^{5,6} This failure is due to the well-known self-interaction error⁷ and the lack of a derivative discontinuity in the exact exchange–correlation (XC) functional of pure DFT.⁸ Correlated wavefunction (CW) methods have been employed to study the interaction of O₂ with several different Al_n clusters in order to go beyond the limitations of DFT.^{9–11} Although a barrier can be observed as O₂ approaches these clusters, this barrier could be an artifact of the finite size of the bare clusters. The origin of the barrier is also under debate. Katz et al.¹² suggested nonadiabatic charge transfer as the origin of the barrier, while Behler et al.^{13,14} attributed the barrier to nonadiabatic spin dynamics and invoked a spin constraint to investigate the problem. Potential energy surfaces (PESs) obtained via the resulting locally spin-constrained DFT formalism using a revised XC functional produced fair agreement with measurements. Recently, Libisch et al. employed an embedded correlated wavefunction (ECW) theory to study the O₂/Al(111) interaction.¹⁵ They found energy barriers naturally emerge without invoking any spin

constraints that are consistent with measurements for all investigated configurations and attributed the barriers' origin to the cost to induce charge transfer from the metal to the oxygen molecule, which is properly captured by CW methods, unlike most DFT approximations.

In addition to reliable barrier height prediction, elucidation of the detailed mechanism by which O₂ interacts with Al(111) is equally important. One scanning tunneling microscopy (STM) study¹⁶ found pairs of oxygen adatoms with interatomic distances on the order of the Al fcc lattice constant at both 80 and 300 K, indicating dissociative chemisorption. By contrast, roughly contemporaneous STM measurements at room temperature consistently found a predominance of isolated adsorbed oxygen atoms formed at low incident O₂ translational energies, implying that the much less exothermic reaction of only adsorbing one oxygen atom (while the other is ejected into the gas phase) counterintuitively dominates at low translational energy (<0.5 eV).^{3,17} These results suggested a lower barrier for dioxygen impinging roughly perpendicular to the surface, an orientation set up to facilitate the abstraction of one oxygen atom by the metal. These contradictory findings left the question about the dominant reaction pathway unsettled, with differing details of the experimental setups also contributing to the uncertainty. In particular, the relative orientations of the molecule and surface are thought to be critically important for determining the outcome of charge-

Received: March 21, 2015

Accepted: April 14, 2015

transfer reactions at metal surfaces.¹⁸ Indeed, recent stereochemical measurements by Kurahashi and Yamauchi¹⁹ found a lower sticking probability for an O₂ beam containing molecules with mostly perpendicular orientation than that for one containing mostly parallel-oriented O₂ molecules, with reaction barriers for the parallel molecules inferred to be 0.1 eV lower than that for the perpendicular case. These direct measurements of steric effects for this system appear to contradict previous observations^{3,17} and call details of the interaction mechanism into question.

Encouraged by the success of the ECW method in providing an explanation for the experimentally observed barrier, here we again apply ECW theory to the O₂/Al(111) system with the aim to settle this controversy. We calculate a set of new PESs for an O₂ molecule approaching the Al(111) surface (see Figure 1a). The high computational expense of ECW calculations

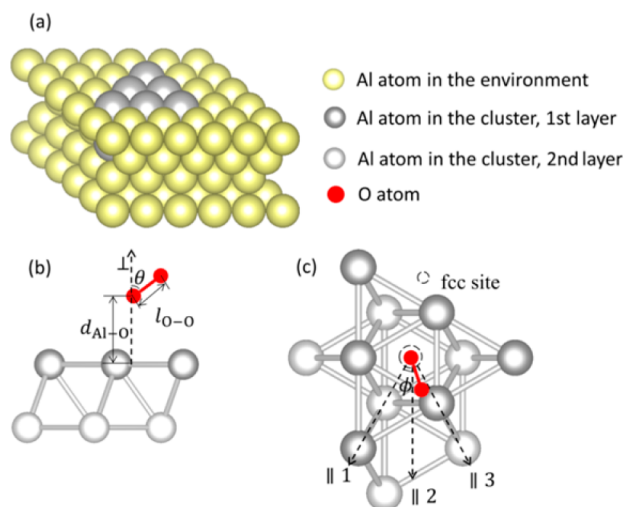


Figure 1. (a) Geometry of the Al slab and (b) side and (c) top views of the Al₁₂ cluster.

prohibits a systematic sampling of the full six-dimensional PES required for a molecular dynamics simulation, which would potentially yield further important insights into the role of orientational degrees of freedom.²⁰ Previous studies were thus restricted to two-dimensional (2D) cuts of the full PES, varying the O–O bond length $l_{\text{O-O}}$ and the O₂–surface distance $d_{\text{Al-O}}$ at perfectly perpendicular and parallel orientations, evaluated at high-symmetry adsorption sites. To go beyond these prior results and understand how the alignment of the O₂ molecule will affect its interaction with the surface, we sample orientational degrees of freedom and various angles of incidence of the approaching O₂ molecule.

A number of embedding schemes have been developed recently to tackle multiphysics problems such as the one discussed here,^{21–24} though the general concepts and developments go back many years.²⁵ In the present work, we use density-functional ECW theory, which has been successfully applied to study metal–surface phenomena.^{26,27} ECW theory combines the high accuracy of CW calculations on clusters with periodic DFT calculations for the extended metal surface.²⁶ It retains the accuracy of CW methods while minimizing, via the embedding procedure, the effect of a limited cluster size. We partition a fcc Al (111) slab, containing four layers in a periodic 5×5 supercell for a total of 100 atoms, into an Al₁₂ cluster, containing six atoms in each of its two layers, and the remaining

environment (see Figure 1a). We use a density-functional embedding theory²⁷ with the PBE XC functional²⁸ to obtain the embedding potential V_{emb} that correctly describes the interaction between the two. Following the same procedure as that in our previous ECW study,¹⁵ the ECW total energy is evaluated as

$$E_{\text{tot}}^{\text{CW,emb}} = E_{\text{tot}}^{\text{DFT}} + (E_{\text{cluster}}^{\text{CW,emb}} - E_{\text{cluster}}^{\text{DFT,emb}}) \quad (1)$$

for various geometries (defined by $l_{\text{O-O}}$, $d_{\text{Al-O}}$, θ , and ϕ ; see Figure 1) to obtain high-dimensional embedded PESs. Here, $E_{\text{tot}}^{\text{DFT}}$ refers to the DFT ground-state energy of the entire system, while $E_{\text{cluster}}^{\text{CW,emb}}$ ($E_{\text{cluster}}^{\text{DFT,emb}}$) are the energies of the embedded cluster using CW (DFT) methods. As in our earlier study,¹⁵ we choose second-order many-body multireference perturbation theory (CASPT2) based on a complete active space self-consistent field (CASSCF) calculation as the CW method of choice (see the Supporting Information for details). The steric effect is investigated around the fcc site of Al(111), which is known to be the most energetically favored adsorption site of the (111) surface.⁵

To investigate the orientation dependence of the barrier to dissociation, we first analyze the adiabatic $d_{\text{Al-O}}$ versus $l_{\text{O-O}}$ 2D cut of the embedded PES at four possible orientations around the fcc site, as illustrated in Figure 1b,c, one perpendicular and three parallel orientations pointing along the directions $[11\bar{2}]$ ($\parallel 1$), $[11\bar{1}]$ ($\parallel 2$), and $[\bar{1}2\bar{1}]$ ($\parallel 3$). For convenience, the closer O atom is constrained to be directly above the fcc site, and $d_{\text{Al-O}}$ is defined as the distance between this O atom and the top layer of the Al₁₂ cluster. All energies are reported relative to a configuration of the O₂ at its equilibrium bond length of 1.25 Å at a distance of 5 Å from the Al₁₂ cluster, where the ECW energy no longer changes with respect to $d_{\text{Al-O}}$ and is independent of the molecule's orientation.

We find energy barriers for all four orientations, associated with the transition states marked by the triangles in Figure 2.

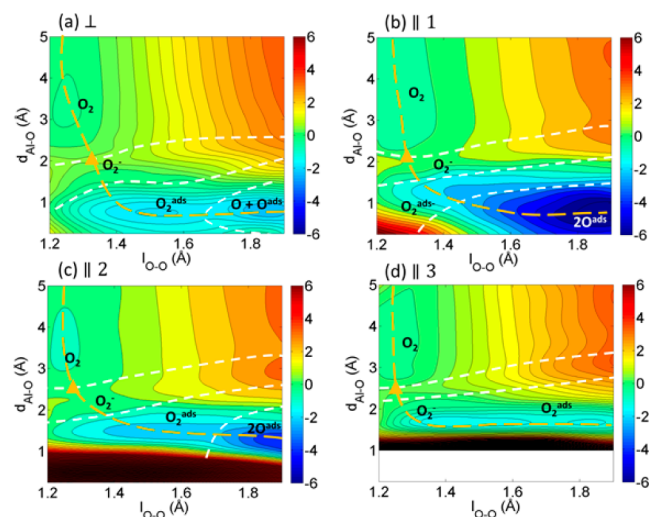


Figure 2. $d_{\text{Al-O}}$ versus $l_{\text{O-O}}$ PESs (energy in eV) of four orientations of the incoming dioxygen molecule (see Figure 1 for definitions). White dashed lines delimit regions of different oxygen charge states, and the yellow dashed line represents the minimum-energy pathway, with the yellow triangle denoting the location of the transition state. O₂[−] denotes the first charge transfer, while O₂^{ads} denotes the second charge transfer, associated with the formation of polar chemical bonds to the closest Al atoms.

The oxygen charge state is determined from the occupation numbers of the CASSCF active orbitals and the CASSCF spin populations on the O atoms. Consistent with our previous work regarding the origin of the barrier,¹⁵ the charge analysis indicates that the transition-state location coincides with the configuration at which the first charge transfer from the surface to the molecule occurs, forming O_2^- for all orientations considered. The barrier heights and $d_{\text{Al-O}_2}^{\text{barrier}}$ for the four orientations are given in Table 1. We find large variations in

Table 1. ECW Prediction of Barrier Heights and Distances between the Parallel O_2 (or the Closer O Atom in Perpendicular O_2) and the Al Surface at the Top of the Barrier ($d_{\text{Al-O}_2}^{\text{barrier}}$) for Four Different O_2 Orientations

	O–O orientation	$d_{\text{Al-O}_2}^{\text{barrier}}$ (Å)	barrier height (eV)
	1: $[11\bar{2}]$	1.9	0.62
	2: $[01\bar{1}]$	2.2	0.45
	3: $[\bar{1}2\bar{1}]$	2.4	0.19
⊥	$[111]$	1.9	0.43

barrier height as a function of alignment of the incoming oxygen molecule. While the perpendicular orientation has a comparatively low barrier, the smallest barrier emerges for || 3 (see Figure 2d). The closer distance between the outer O atom and a surface Al atom in the || 3 geometry (see Figure 1c) directly results in a larger amount of orbital overlap than other configurations. This larger overlap facilitates the charge-transfer process, leading to the lowest barrier height and the largest $d_{\text{Al-O}_2}^{\text{barrier}}$. By contrast, the orientation of || 1 corresponds to the highest barrier, consistent with our earlier study.¹⁵ DFT-GGA investigations with the revised PBE XC functional^{5,6} predicted that the bri-v configuration (where the O_2 center-of-mass is on top of the bridge site with the O–O axis in the $[11\bar{2}]$ direction, as in || 1) is the only one with a nonzero activation barrier, which qualitatively agrees with the barrier height ordering that we obtain here. The additional parallel orientation cases considered here, varying the azimuthal angle beyond the one examined in ref 15, reveals that || 3 has an activation barrier even lower than the perpendicular orientation. The difference in barrier height between parallel and perpendicular orientations (~ 0.2 eV) is, within the accuracy of our model and experimental error bars, consistent with the latest experimental data of Kurahashi and Yamauchi (~ 0.1 eV).¹⁹

The charge state of the oxygen molecule after crossing the barrier is determined as described above. The four PESs are qualitatively similar around the barrier, where the first charge transfer results in an O_2^- ion that then becomes chemically bound to the surface in a second charge transfer (denoted by O_2^{ads} in Figure 2). However, the orientation of the molecule has a strong impact on the topology of the PESs after the initial charge transfer. For the perpendicular orientation, a local energy minimum (Figure 2a) located at $d_{\text{Al-O}} = 0.75$ Å corresponds to an intermediate state of molecularly adsorbed O_2^{ads} . Further elongation of the O–O bond length finally leads to one abstracted O atom and one adsorbed O^{ads} , as reported earlier.¹⁵ For the parallel orientations || 1 and || 2, the reaction pathway goes downhill energetically as the O–O bond stretches, ultimately resulting in a pair of adsorbed O^{ads} , that is, in dissociative chemisorption (Figure 2b,c). || 1 connects to adsorption at adjacent fcc and hcp sites, while || 2 connects to adsorption at a pair of neighboring fcc sites, which is

energetically slightly preferred (as we have verified by extending the PESs of Figure 2 to larger O–O bond length; see Supporting Information Figure S1). The relative energies of the two adsorption configurations are consistent with previous DFT-GGA calculations.⁵ For || 3, though, after formation of O_2^{ads} , the energy abruptly increases upon approach to the surface due to the strong repulsion between the charged O atom and the Al atom underneath. Evolution toward an fcc-(over atop site)-hcp pair adsorption state (see Figure 1c) in combination with an O–O bond stretch does not appear kinetically favorable. Instead, comparing the PESs for || configurations 2 and 3 at $d_{\text{Al-O}} \approx 1.0$ Å (Figure 2c,d) suggests that a rotation from || 3 to || 2 could substantially lower the energy (by ~ 5 eV). Because the lowest-barrier channel with || 3 orientation does not directly connect to a stable final state on the 2D PES depicted in Figure 2, the oxygen molecule may adjust itself in the interaction process to stick to a minimum-energy reaction path.

We therefore further relax the orientational degrees of freedom of the oxygen molecule by examining a variety of azimuthal (ϕ) and tilt angles (θ) (see Figure 1) for different $d_{\text{Al-O}}$ with a fixed $l_{\text{O-O}} = 1.3$ Å. Although this is not the exact equilibrium bond length of the O_2 molecule, the topology of the PES is not affected by the slight difference in $l_{\text{O-O}}$ value.

When O_2 is 2.5 Å away from the Al surface, two local minima exist (see triangles in Figure 3a). Among the parallel cases

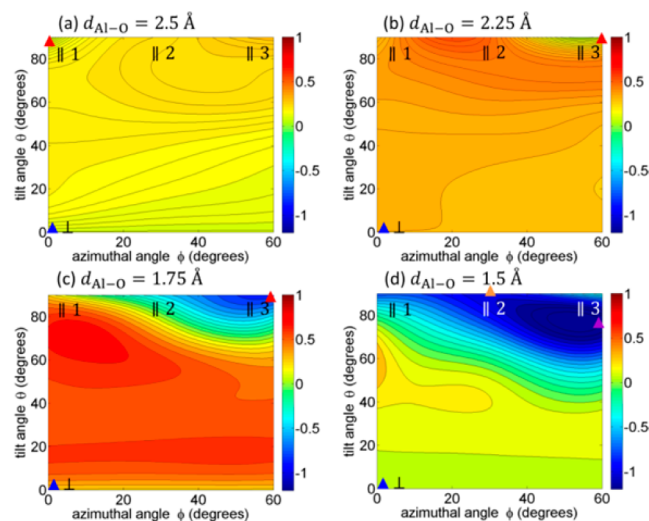


Figure 3. θ versus ϕ PESs with $l_{\text{O-O}} = 1.3$ Å (energy in eV) at four $d_{\text{Al-O}}$ (distances between the closer O atom and the Al surface). The triangles denote important energy minima (either local or global) on the PESs.

(large tilt angle, top of each panel in Figure 3), the bridge-site-like orientation (|| 1, red triangle) is energetically favored. For small tilt angles (bottom of each panel in Figure 3), the local minimum corresponds to the perpendicular orientation (blue triangle). This PES cut suggests that an incoming molecule with low translational energy may rotate toward one of the two nearby local minima. Thus, a substantial portion of the tilted O_2 molecules, namely, those within a cone-shaped region delimited by a tilt angle of $\sim 70^\circ$ (see Figure 3a), will rotate upright, while the rest will align along the || 1 direction. A previous DFT-GGA-based study⁵ also observed that O_2 molecules tend to orient themselves perpendicular to the surface. As the molecule approaches the surface more closely (at $d_{\text{Al-O}} = 2.25$ Å), charge

transfer can happen around the $\parallel 3$ orientation, resulting in a new local minimum on the θ versus ϕ PES. The lower barrier height accompanied by a charge transfer should rotate the oxygen molecule away from the $\parallel 1$ direction toward the $\parallel 3$ direction. Meanwhile, the perpendicular orientation still remains a local minimum. This energy ordering holds up to a shorter distance of $d_{\text{Al-O}} = 1.5 \text{ \AA}$, where O_2^{ads} is formed for all three parallel configurations. The large amount of overlap between the $\text{O}_2 \pi^*$ and Al surface orbitals in the $\parallel 3$ direction induces an energy increase (see Figure 2d at $d_{\text{Al-O}} < 1.5 \text{ \AA}$). Concurrently, $\parallel 2$ becomes one of the local minima (denoted by a yellow triangle in Figure 3d), which ultimately evolves to the most energetically favored final state, neighboring fcc/fcc site adsorption. Thus, rotating within the plane from $\parallel 3$ to $\parallel 2$ is an efficient way to relax the geometry. Another local minimum at $\theta = 75^\circ$ and $\phi = 60^\circ$ (denoted by the purple triangle in Figure 3d) corresponds to the O_2 molecule tilting out of the plane from the $\parallel 3$ direction. This is yet another pathway toward relaxing the energetically unfavored geometry in $\parallel 3$.

To confirm the validity of these two proposed relaxation pathways away from $\parallel 3$ after charge transfer, we investigate the evolution of the lowest-barrier channel ($\parallel 3$) as a function of tilt angle and bond length. We find a local minimum that slowly evolves toward smaller tilt angles and larger O–O bond lengths as the molecule approaches the surface (compare Figure 4a,b).

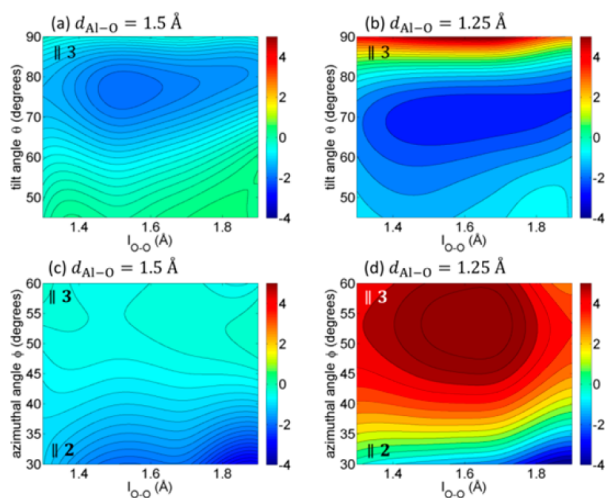


Figure 4. (a,b) θ versus $l_{\text{O-O}}$ PES (energy in eV) with $\phi = 60^\circ$ (tilted $\parallel 3$ direction) and $d_{\text{Al-O}}$ as marked; (c,d) ϕ versus $l_{\text{O-O}}$ PES (energy in eV) with $\theta = 90^\circ$ (\parallel) and $d_{\text{Al-O}}$ as marked.

Such a trend suggests that the molecule tends to tilt upward with O–O bond elongation and ends up in an abstractive adsorption state. On the ϕ versus $l_{\text{O-O}}$ PES with $\theta = 90^\circ$ (see Figure 4c,d), the energy minimum at $\phi \approx 30^\circ$ and $l_{\text{O-O}} \approx 1.9 \text{ \AA}$ in both PESs clearly confirms that rotation within the plane toward $\parallel 2$ to avoid strong electron repulsion is another possible reaction path. Thus, we see that multiple reaction pathways can compete, resulting in the coexistence of single adsorbed O atoms and pairs of adjacent, adsorbed O atoms.

It is essential to consider stereochemistry along the reaction path to elucidate the detailed mechanism of how O_2 interacts with Al(111). First, a distribution of O_2 molecule alignments must be taken into account while determining barrier heights for the reaction. Our PES cuts demonstrate that the barrier

depends strongly on both the tilt and azimuthal angles of the O_2 with respect to the surface. We find that certain parallel orientations may indeed dominate at low translational energy, in agreement with a recent experimental study of the steric effect. Second, by relaxing the orientational degrees of freedom, we are able to connect the lowest-barrier-height reaction channel to the two major final states. The minimum-energy reaction path begins with a parallel orientation that undergoes the easiest charge transfer. However, the molecule experiences a strong torque immediately after charge transfer, resulting in either abstraction by tilting upright or dissociative adsorption at neighboring fcc sites by rotating toward a more favorable parallel configuration. This mechanism raises the possibility that the oxygen molecule with parallel incidence ultimately evolves into one adsorbed (abstracted) O atom and one ejected O atom, consistent with earlier measurements. These two conclusions drawn from the systematic analysis of various cuts of PESs thus reconcile two seemingly contradictory experimental findings. However, current adiabatic PES cuts cannot provide solid evidence to explain why the abstraction channel dominates over the dissociative adsorption channel after crossing the barrier. We hope that future molecular dynamics studies based on our PESs can shed further light on this issue.

■ ASSOCIATED CONTENT

📄 Supporting Information

Computational details of the embedded correlated wavefunction method, extended potential energy surfaces for the dissociative adsorption state, and the error estimation. This material is available free of charge via the Internet at <http://pubs.acs.org>.

■ AUTHOR INFORMATION

Corresponding Author

*E-mail: eac@princeton.edu.

Notes

The authors declare no competing financial interest.

■ ACKNOWLEDGMENTS

We are grateful for support of this research from the U.S. National Science Foundation under Award No. 1265700 (E.A.C.) and to the Austrian Science Fund (FWF) under SFB-041 VICOM (F.L.).

■ REFERENCES

- (1) Kroes, G.-J. *Frontiers in Surface Scattering Simulations*. *Science* **2008**, *321*, 794–797.
- (2) Österlund, L.; Zoric-acute, I.; Kasemo, B. Dissociative Sticking of O_2 on Al(111). *Phys. Rev. B* **1997**, *55*, 15452–15455.
- (3) Komrowski, A.; Sexton, J.; Kummel, A.; Binetti, M.; Weiße, O.; Hasselbrink, E. Oxygen Abstraction from Dioxygen on the Al(111) Surface. *Phys. Rev. Lett.* **2001**, *87*, 246103.
- (4) Binetti, M.; Hasselbrink, E. Abstraction of Oxygen from Dioxygen on Al(111) Revealed by Resonant Multiphoton Ionization Laser Spectrometry. *J. Phys. Chem. B* **2004**, *108*, 14677–14684.
- (5) Yourdshahyan, Y.; Razaznejad, B.; Lundqvist, B. Adiabatic Potential-Energy Surfaces for Oxygen on Al(111). *Phys. Rev. B* **2002**, *65*, 075416.
- (6) Honkala, K.; Laasonen, K. Oxygen Molecule Dissociation on the Al(111) Surface. *Phys. Rev. Lett.* **2000**, *84*, 705–708.
- (7) Perdew, J. P. Self-Interaction Correction to Density-Functional Approximations for Many-Electron Systems. *Phys. Rev. B* **1981**, *23*, 5048–5079.

- (8) Perdew, J. P.; Levy, M.; Balduz, J. L. Density-Functional Theory for Fractional Particle Number: Derivative Discontinuities of the Energy. *Phys. Rev. Lett.* **1982**, *49*, 1691–1694.
- (9) Bacalis, N. C.; Metropoulos, A.; Gross, A. Theoretical Study of the O₂ Interaction with a Tetrahedral Al₄ Cluster. *J. Phys. Chem. A* **2010**, *114*, 11746–11750.
- (10) Mosch, C.; Koukounas, C.; Bacalis, N.; Metropoulos, A.; Gross, A.; Mavridis, A. Interaction of Dioxygen with Al Clusters and Al(111): A Comparative Theoretical Study. *J. Phys. Chem. C* **2008**, *112*, 6924–6932.
- (11) Livshits, E.; Baer, R.; Kosloff, R. Deleterious Effects of Long-Range Self-Repulsion on the Density Functional Description of O₂ Sticking on Aluminum. *J. Phys. Chem. A* **2009**, *113*, 7521–7527.
- (12) Katz, G.; Kosloff, R.; Zeiri, Y. Abstractive Dissociation of Oxygen over Al(111): A Nonadiabatic Quantum Model. *J. Chem. Phys.* **2004**, *120*, 3931–3948.
- (13) Behler, J.; Delley, B.; Lorenz, S.; Reuter, K.; Scheffler, M. Dissociation of O₂ at Al(111): The Role of Spin Selection Rules. *Phys. Rev. Lett.* **2005**, *94*, 036104.
- (14) Behler, J.; Reuter, K.; Scheffler, M. Nonadiabatic Effects in the Dissociation of Oxygen Molecules at the Al(111) Surface. *Phys. Rev. B* **2008**, *77*, 115421.
- (15) Libisch, F.; Huang, C.; Liao, P.; Pavone, M.; Carter, E. A. Origin of the Energy Barrier to Chemical Reactions of O₂ on Al(111): Evidence for Charge Transfer, Not Spin Selection. *Phys. Rev. Lett.* **2012**, *109*, 198303.
- (16) Schmid, M.; Leonardelli, G.; Tscheließnig, R.; Biedermann, A.; Varga, P. Oxygen Adsorption on Al(111): Low Transient Mobility. *Surf. Sci.* **2001**, *478*, L355–L362.
- (17) Binetti, M.; Weiße, O.; Hasselbrink, E.; Komrowski, A. J.; Kummel, A. C. Abstractive Chemisorption of O₂ on Al(111). *Faraday Discuss.* **2000**, *117*, 313–320.
- (18) Bartels, N.; Golibrzuch, K.; Bartels, C.; Chen, L.; Auerbach, D. J.; Wodtke, A. M.; Schäfer, T. Observation of Orientation-Dependent Electron Transfer in Molecule–Surface Collisions. *Proc. Natl. Acad. Sci. U.S.A.* **2013**, *110*, 17738–17743.
- (19) Kurahashi, M.; Yamauchi, Y. Steric Effect in O₂ Sticking on Al(111): Preference for Parallel Geometry. *Phys. Rev. Lett.* **2013**, *110*, 246102.
- (20) Evans, J. W.; Liu, D.-J. Statistical Mechanical Models for Dissociative Adsorption of O₂ on Metal(100) Surfaces with Blocking, Steering, and Funneling. *J. Chem. Phys.* **2014**, *140*, 194704.
- (21) Severo Pereira Gomes, A.; Jacob, C. R. Quantum-Chemical Embedding Methods for Treating Local Electronic Excitations in Complex Chemical Systems. *Annu. Rep. Prog. Chem., Sect. C: Phys. Chem.* **2012**, *108*, 222.
- (22) Jacob, C. R.; Neugebauer, J. Subsystem Density-Functional Theory. *Wiley Interdiscip. Rev. Comput. Mol. Sci.* **2014**, *4*, 325–362.
- (23) Goodpaster, J. D.; Barnes, T. A.; Manby, F. R.; Miller, T. F. Density Functional Theory Embedding for Correlated Wavefunctions: Improved Methods for Open-Shell Systems and Transition Metal Complexes. *J. Chem. Phys.* **2012**, *137*, 224113.
- (24) Daday, C.; König, C.; Valsson, O.; Neugebauer, J.; Filippi, C. State-Specific Embedding Potentials for Excitation-Energy Calculations. *J. Chem. Theory Comput.* **2013**, *9*, 2355–2367.
- (25) Huang, P.; Carter, E. A. Advances in Correlated Electronic Structure Methods for Solids, Surfaces, and Nanostructures. *Annu. Rev. Phys. Chem.* **2008**, *59*, 261–290.
- (26) Libisch, F.; Huang, C.; Carter, E. A. Embedded Correlated Wavefunction Schemes: Theory and Applications. *Acc. Chem. Res.* **2014**, *47*, 2768–2775.
- (27) Huang, C.; Pavone, M.; Carter, E. A. Quantum Mechanical Embedding Theory Based on a Unique Embedding Potential. *J. Chem. Phys.* **2011**, *134*, 154110.
- (28) Perdew, J. P.; Burke, K.; Ernzerhof, M. Generalized Gradient Approximation Made Simple. *Phys. Rev. Lett.* **1996**, *77*, 3865–3868.